

## CHAPTER 5. PHASE SHIFTER SYNTHESIS

### 5.1. Introduction

For completeness, it was decided to synthesize a  $45^\circ$  phase shifter, due to the sensitivity analysis highlighting it as the most sensitive to tolerance variations. Firstly, a general synthesis procedure is presented to aid future designers in realising any ultra-broadband phase shifter of the newly proposed type. Restrictions to the developed theory are also highlighted. Critical manufacturing requirements and process tolerances are discussed to provide a feel for the ability to manufacture large quantities of these devices. Well-known state-of-the-art materials are chosen and the trade-offs are discussed. From a typical electrical performance specification, the device is designed and realised. The theoretical and measured performance figures are then presented and compared.

### 5.2. General Phase Shifter Synthesis Guidelines

The design of a wideband phase shifter starts with a specification of phase shift, ripple and bandwidth. The synthesis is restricted to homogeneous triplate media such as PTFE stripline structures, for optimum bandwidth.

- The mean and ripple coupling values of the coupler are calculated from the specification, using the phase shifter transform equations. If the coupling exceeds about 6 dB, two or more couplers should be used in tandem to relax the coupling specification per coupler. To simplify the design, tandem connected couplers are chosen to be identical. For phase shifts lower than  $45^\circ$ , an odd number of couplers is recommended to de-sensitize the phase shifter to tolerance variations. For phase shifts higher than  $45^\circ$ , an even number of tandem-connected couplers is recommended.
- For narrow-band or low frequency phase shifters, it is not always necessary to taper the couplers continuously. For wideband and high frequency operation, (eg exceeding 10 GHz) Tresselt's continuously tapered coupler principles [1] should be applied to improve directivity. Select the spacing  $s$  to be as small as possible (eg 5 mil) to minimize the via lengths and improve splitter performance. The ground plane spacing  $b$  is selected to best fit the fixed coupling value at the centre of the couplers for an internal impedance of  $50 \Omega$ . The couplers are then designed as discussed in Section 3.3.

- Exponential tapers are easily designed as in Section 3.2.2 and were found to be very successful, since taper performance is very insensitive to tolerance as calculated in Section 3.2.3. However, any taper, for example the Hecken taper, can be applied successfully.
- To design the splitter, calculate the BCS splitter width from Cohn's equations as discussed in Chapter 3. Choose the via diameter to be about half this width to avoid fringe field interference. The spacing of the vias should be selected to be as low as possible to avoid in-band resonance as discussed in Section 3.4.4.4 (typically 2mm). For frequencies below 10 GHz, two or three vias should be sufficient. Use of four vias extends the splitter performance to the millimetre wave band.

The via analysis reveals that small changes in via nature does not affect the performance of the splitter. The most typical material choices were used in the thorough analysis of the via splitter, but other materials are also expected to yield acceptable splitter results. To ensure smooth transitions between the elements comprising the phase shifter, it is important to avoid additional parasitical components internal to the phase shifter which could add to asymmetry.

### 5.3. Processes and Tolerance Requirements

A material that is very commonly used in the industry for accurate stripline microwave components, is the well-known RT/Duroid 5880 glass fibre reinforced polytetrafluoroethylene (PTFE) composite supplied by Rogers corporation. The fibres are randomly oriented to ensure a highly homogeneous substrate, and the dielectric constant is also found to be constant from panel to panel, over a wide frequency range. The substrate also has excellent machinability.

The dielectric constant of RT/Duroid 5880 composite is  $2.2 \pm 0.02$  at 10 GHz at a temperature of 30°C and has a 0.78% tolerance at 0°C and 100°C. Therefore it is expected that the taper performance will not be affected significantly by temperature variations. All lines will have an added reflection coefficient of less than -45 dB and the bandwidth of the coupler (and therefore of the phase shifter) may change by a maximum of 200 MHz at 20 GHz. The material loss factor ( $\tan \delta$ ) is specified at 0.0009 at 10 GHz, which is very low. Regarding the substrate thickness tolerances, the 5 mil centre slab thickness  $s$  is expected to be within 13  $\mu\text{m}$  and the GPS within 64  $\mu\text{m}$ . Again the lines and tapers are virtually unaffected but the combined worst case may cause a coupling deviation



of 0.24 dB and a bandwidth change of 300 MHz at 20 GHz. While it is difficult to verify the dielectric constant, measured substrate thickness should be used in design calculations.

The expected copper thickness  $t$  is  $18\mu\text{m}$ . The copper can be either rolled foil or electro-deposited onto the PTFE. Electro-deposited copper is prone to thermal stress cracks, especially for thin lines, but has a better adhesion to PTFE than rolled copper foil. Since it is desired to etch high-impedance lines accurately, rolled copper proves to be the better choice, especially since the surface roughness of rolled copper is the lowest. A roughness of  $1.4\mu\text{m}$  is expected, causing a 0.03 dB coupling value deviation in the coupler. Rolled copper also has much lower losses at high frequencies. The lines and taper are only slightly affected.

Over- or under-etching of  $25\mu\text{m}$  can cause a 0.45 dB coupling error, and should be compensated for by adding line-width to the mask. A  $10\mu\text{m}$  accuracy can be expected, leading to a 0.18 dB coupling tolerance. Scaling errors of 5% can also cause a 0.48 dB coupling tolerance, but less than 0.05% scaling error can be expected when the mask is laser-plotted and scaling verified by microscope. The top and bottom etch mask alignment at the photolithographic process proves to be the critical factor. Linear alignment errors of  $70\mu\text{m}$  and rotational errors of  $1^\circ$  cause 0.6 dB and 0.8 dB coupling errors respectively and  $5.6^\circ$  and  $0.3^\circ$  of phase errors respectively.

The splitter performance, as discussed previously, can be expected to be within 0.4 dB and  $3^\circ$  providing that the vias are realised by bonding gold ribbons through the via holes and filling the through holes with conductive epoxy.

Considering all processes and the associated tolerances, a coupler coupling error of about 0.8 dB and phase accuracy of  $8.5^\circ$  can be expected. These figures dominate the phase shifter performance, and a phase shift accuracy of  $0.7^\circ$  and amplitude deviation of 0.15 dB can be expected.

#### 5.4. Phase Shifter Practical Example

As an example, a  $45^\circ \pm 5^\circ$  phase shifter over a 2-18 GHz band will be synthesised. The coupling for  $45^\circ$  phase shift can be calculated by equation (2.22).

$$\begin{aligned} C_0 \text{ (dB)} &= 20 \log[\sin 45^\circ] \\ &= -3.01 \text{ dB} \end{aligned} \quad (5.1)$$

The phase ripple is  $\pm 5^\circ$ . The corresponding coupling ripple is then, according to equation (2.24)

$$\delta_0 \text{ (dB)} = 20 \log \left[ \frac{\sin (45^\circ + 5^\circ)}{\sin (45^\circ)} \right] = 0.695 \text{ dB} . \quad (5.2)$$

Since the mean coupling  $C_0$  is too tight for a single coupler, the tandem connection of two identical couplers may be implemented, their coupling and ripple values being

$$C_0 \text{ (dB)} = 20 \log [\sin (22.5^\circ)] = -8.343 \text{ dB} , \quad (5.3)$$

$$\delta_0 = 20 \log \left[ \frac{\sin (22.5^\circ + 2.5^\circ)}{\sin (22.5^\circ)} \right] = 0.862 \text{ dB} . \quad (5.4)$$

When designing coupler sections for optimal performance, it was found that a 5-section coupler will meet these specifications. The optimal normalized impedance levels as calculated by the optimization program described in section 3.3.1, were found to be

$$Z_1 = 1.09218 ,$$

$$Z_2 = 1.26492 ,$$

$$Z_3 = 2.09984 .$$

The coupler design program described in paragraph 3.3.1 was run to synthesize the coupler. Typical measured  $s$ -parameter results of a 9-section test coupler is shown in Appendix E. The computer text file of the synthesis of the phase shifter coupler is also found in Appendix E. The graphical file which is also generated by the design program was stored to generate the etch-mask.

The splitter width was found to be 0.602 mm to ensure a  $100 \Omega$  even-mode impedance. A 0.3 mm diameter was chosen, causing a 29.03 pH and  $-357.2 \mu\text{m}$  phase model for the via. The via spacing should be less than 5.06 mm to avoid resonance. Four vias were chosen with a 2 mm spacing.

The results of the sensitivity analysis are applied to the example in the last chapter to obtain acceptable splitter-coupler-taper imbalance and asymmetry tolerance figures for a desired phase shifter performance. Alternatively, the measured amplitude and phase tolerance of the practical phase shifter may be applied to the sensitivity analysis equations to quantify achieved imbalance.

In the practical example case, two tandem-connected couplers are synthesized to yield a  $45^\circ$  phase shifter. The equations for the even number of tandem-connected couplers are used at  $45^\circ$ .

$$S = \sin [ 2 \arctan (10^{\delta/20}) ] \quad , \quad (5.5)$$

$$C = \cos [ 2 \arctan (10^{\delta/20}) ] \quad . \quad (5.6)$$

where  $\delta$  represents the amplitude imbalance, in dB. Let  $\theta$  be the phase imbalance of the phase shifter. Then the associated amplitude and phase errors are

$$P_e (\delta, \theta) = 20 \log \left[ \frac{\cos^2 \theta + (S_D - C_D \sin \theta)^2}{2} \right] \quad , \quad (5.7)$$

$$\Psi_e (\delta, \theta) = \arctan \left[ \frac{\cos \theta - S_D + C_D \sin \theta}{\cos \theta + S_D - C_D \sin \theta} \right] \quad . \quad (5.8)$$

The results are presented graphically, for  $-40^\circ < \theta < 40^\circ$  and  $\delta = 1, 2, 3$  dB in Figures 32 and 34.

The next table summarises the results for up to three vias:

**Table 5.1 : Expected performance of phase shifters with up to 3 vias**

Via No.	$\theta$ (deg)	$\delta$ (dB)	A err (dB)	$\Psi$ err (deg)
1	7.5	15	2	8
2	5	6	0.4	3
3	2.5	3	0.3	2

An improved grasp of performance deviations that can be expected for a certain imbalance caused by manufacturing tolerance, was obtained. The sensitivity analysis was applied to the practical phase shifter example. The phase shifter seems to be fairly insensitive to manufacturing tolerances.



The tapers were synthesised as described by section 3.2.1. The photomask of the phase shifter is shown in Figure 35. Compensation of  $35\ \mu\text{m}$  was added to the line width to counteract the effect of over-etching.

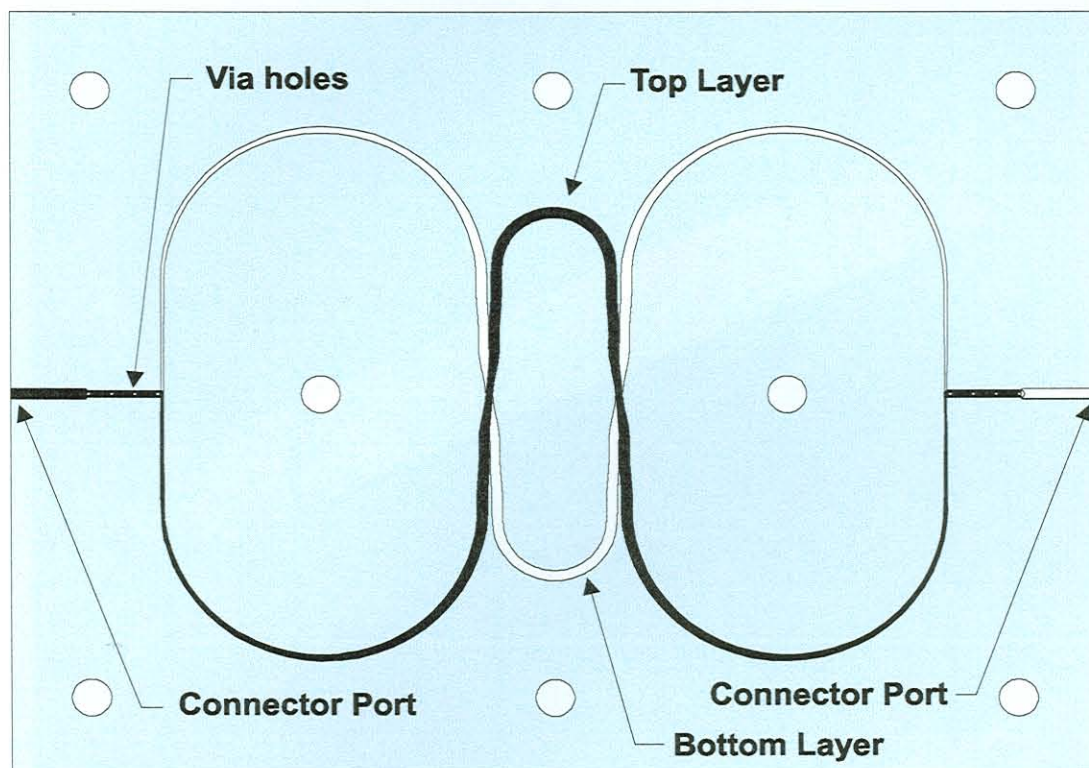


**Figure 35 : Photomask of a  $45^\circ$  phase shifter**

### 5.5. Practical Phase Shifter Results

The practical results of the phase shifter synthesized in 5.4 are now briefly discussed. Figure 36 shows a 20 : 1 microscope photo of the splitter, and a closer 50 : 1 photo of a ribbon-epoxy constructed via.

The sharp edge definition and  $25\ \mu\text{m}$  tolerance suggests an excellent etching process control. The gold ribbons were mounted and the epoxy filled in a class 100 cleanroom.

A photo of the pre-assembled phase shifter is shown in Figure 37. The  $100\text{-}50\ \Omega$  tapered transformer lines and tandem-connected couplers can clearly be seen. To prevent corrosion, a flush of gold was plated on the circuit tracks.

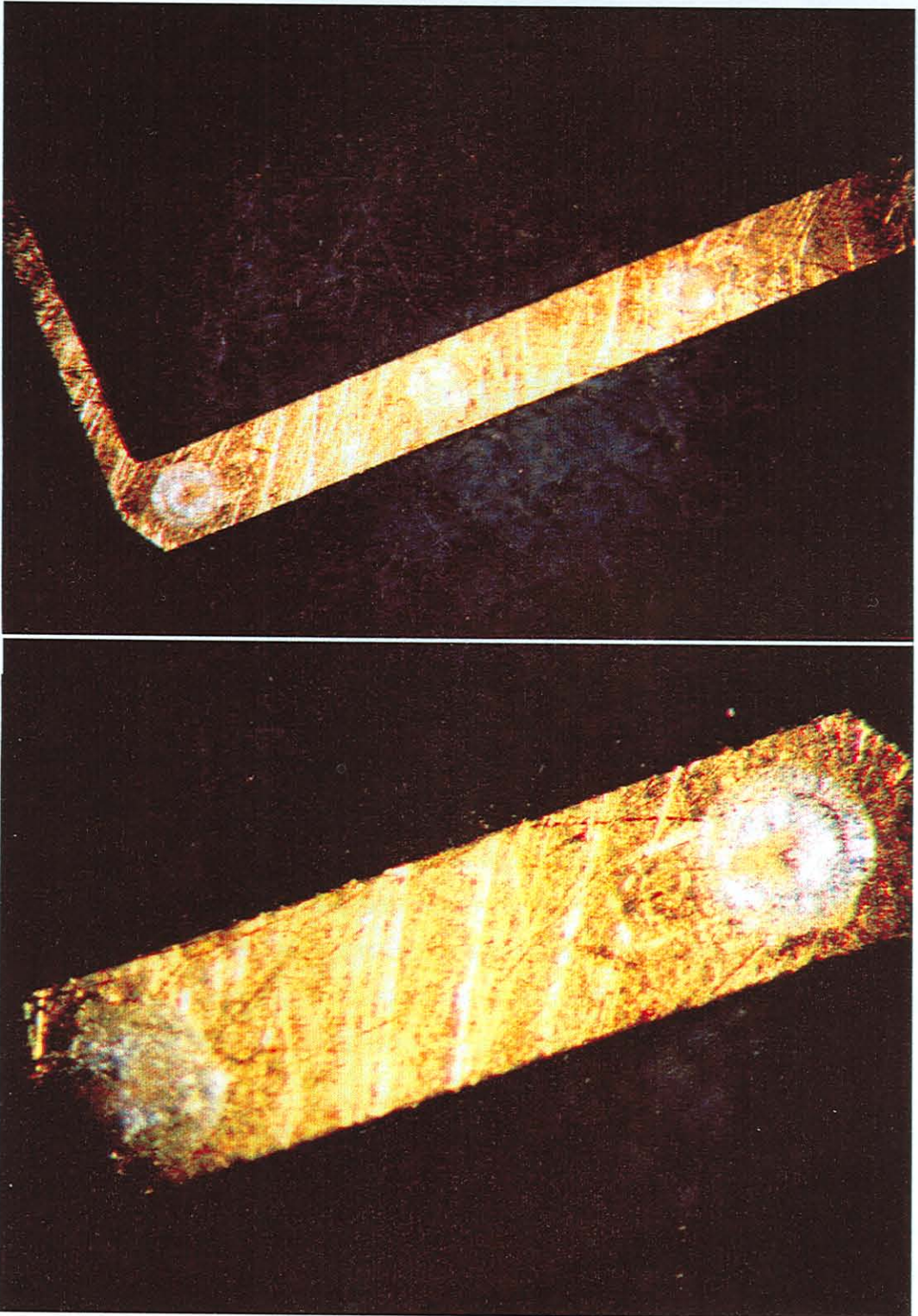


**Figure 36 : The practical splitter and via**



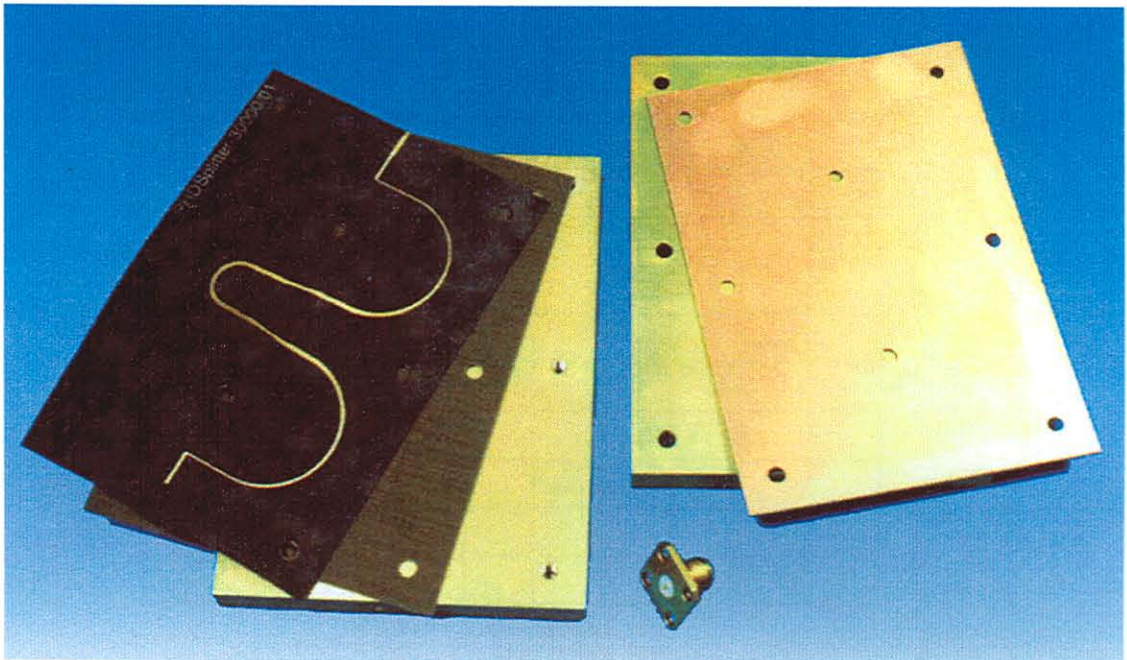


**Figure 37 : The practical phase shifter**

To measure the electrical performance of the phase shifter, the “through” calibration was done including the connectorized reference line, but measurements were conducted by substitution of the reference line by the phase shifter. The theoretical and measured phase shift versus frequency responses are superimposed on one graph (Figure 38). The excellent agreement of these responses demonstrate the theory to be very accurate. From Figure 38 it can be seen that the theoretical and practical phase shift agrees to within three degrees in the 2-18 GHz range. The sensitivity and tolerance analysis can be applied to this specific case and a graph of the expected production tolerance can be generated as in Figure 39. The measured phase shift response is superimposed on this graph to demonstrate the validity of the analysis, and the practicality of the novel phase shifter.

For completeness, Figure 40 shows the measured reflection and insertion loss response of the phase shifter. The results also agree with expected values. The reflection coefficient is below -15dBc from 2-18GHz except for the peak at 2.5GHz, and the maximum loss is only 1.7dB at 18GHz. The 0.602 mm lines in the 100  $\Omega$  tapered lines contribute most of the losses experienced at high frequency.



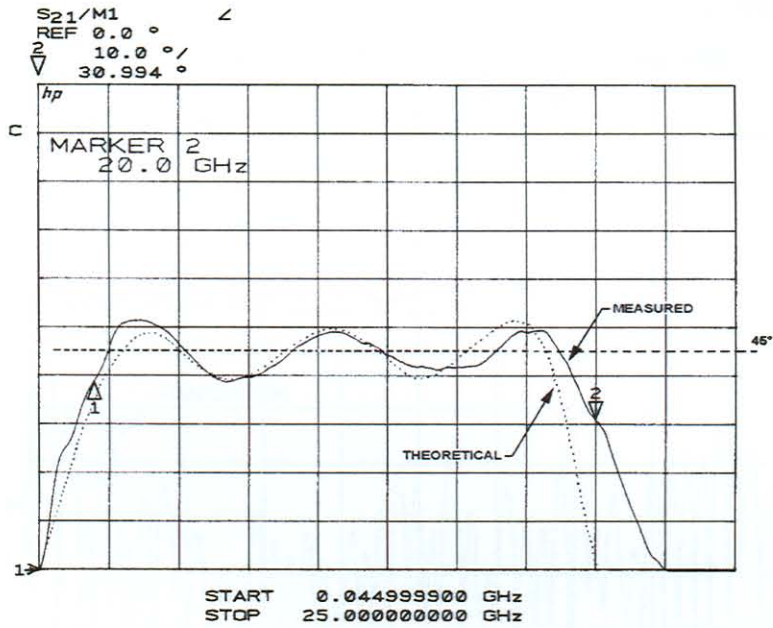


Figure 38 : Measured and theoretical phase shift response

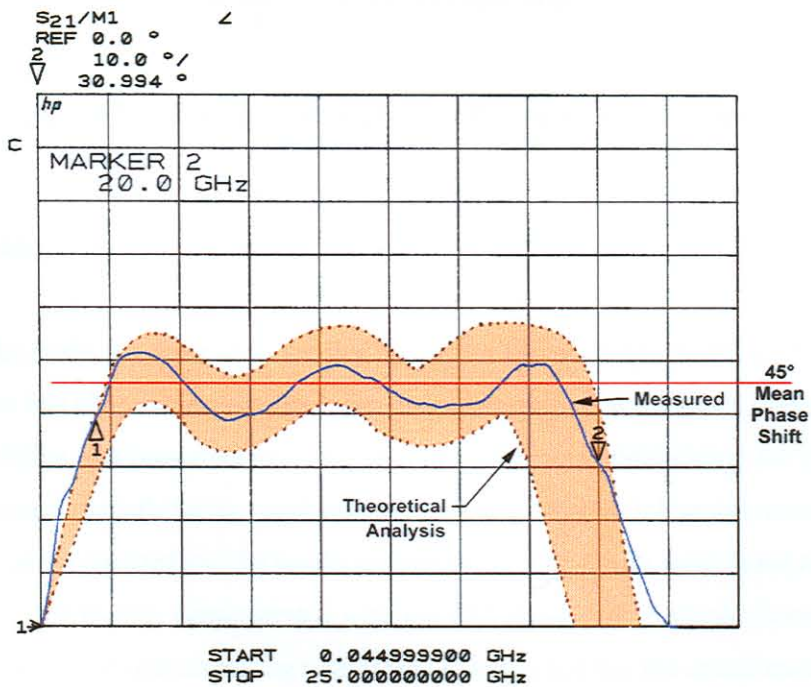
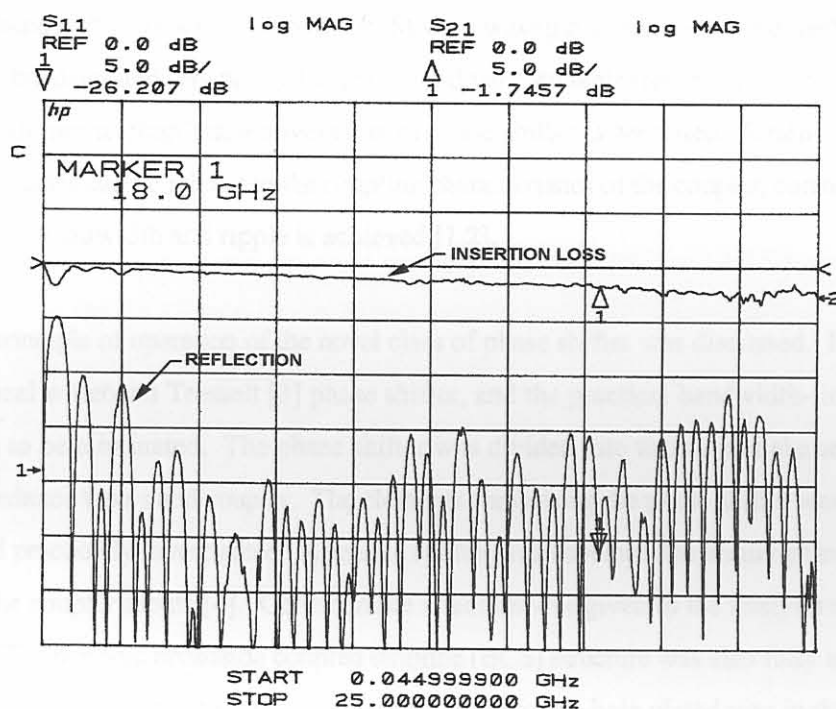


Figure 39 : Measurement and expected production tolerance of the phase shift response



**Figure 40 : Measured reflection and insertion loss response**

## 5.6. Conclusion

To complete the study, the theory was verified by a phase shifter design example. A  $45^\circ$  phase shifter was chosen, as this phase shift provides a device most sensitive to tolerance variations. A general synthesis guideline was presented as an aid to future designers, highlighting the restrictions to the synthesis. Practical manufacturing requirements and typical process tolerances were discussed. The phase shifter was synthesized and the results are presented. The results were found to be in very close agreement with the theory, demonstrated with the  $45^\circ$  phase shifter which proved to be the most sensitive to material and manufacturing tolerances. It was found that the actual measured results fall within the analytical tolerance boundaries. Practically, the bandwidth was found to be slightly wider than predicted due to a combination of dielectric tolerance and scaling error. The in-band phase shift exceeded the  $5^\circ$  ripple at the first 2 ripple points by about one degree. Practically, the phase shift ripple value should therefore be chosen somewhat smaller than the specification. It can be expected that phase shift performance will be better at phase shift values further away from  $45^\circ$ .